

Therapeutic Effects of Simultaneous Delivery of Nerve Growth Factor mRNA and Protein via Exosomes on Cerebral Ischemia

Jialei Yang,^{1,2,3,5} Shipo Wu,^{3,5} Lihua Hou,³ Danni Zhu,³ Shimin Yin,² Guodong Yang,⁴ and Yongjun Wang¹

¹China National Clinical Research Center for Neurological Diseases, Beijing 100070, China; Department of Neurology, Beijing Tiantan Hospital, Capital Medical University, Beijing 100070, China; ²Department of Neurology, PLA Rocket Force Characteristic Medical Center, Beijing, China; ³Beijing Institute of Biotechnology, Beijing, China; ⁴Department of Biochemistry and Molecular Biology, Fourth Military Medical University, Xi'an, Shaanxi 710032, China

Stroke is the leading neurological cause of death and disability all over the world, with few effective drugs. Nerve growth factor (NGF) is well known for its multifaceted neuroprotective functions post-ischemia. However, the lack of an efficient approach to systemically deliver bioactive NGF into ischemic region hinders its clinical application. In this study, we engineered the exosomes with RVG peptide on the surface for neuron targeting and loaded NGF into exosomes simultaneously, with the resultant exosomes denoted as NGF@Exo^{RVG}. By systemic administration of NGF@Exo^{RVG}, NGF was efficiently delivered into ischemic cortex, with a burst release of encapsulated NGF protein and *de novo* NGF protein translated from the delivered mRNA. Moreover, NGF@Exo^{RVG} was found to be highly stable for preservation and function efficiently for a long time *in vivo*. Functional study revealed that the delivered NGF reduced inflammation by reshaping microglia polarization, promoted cell survival, and increased the population of doublecortin-positive cells, a marker of neuroblast. The results of our study suggest the potential therapeutic effects of NGF@Exo^{RVG} for stroke. Moreover, the strategy proposed in our study may shed light on the clinical application of other neurotrophic factors for central nervous system diseases.

INTRODUCTION

According to global burden of disease study, stroke is the leading neurological cause of death and disability all over the world.¹ The only Food and Drug Administration-licensed pharmacological treatment for acute ischemic stroke is recombinant tissue plasminogen activator (rt-PA). However, due to the narrow therapeutic window of 4.5 h, only a minority of patients can benefit from rt-PA therapy for the restoration of cerebral blood flow.² There remains an unmet need for comprehensive neuroprotective strategies to reduce ischemic injury.

In the early 1950s, nerve growth factor (NGF) was discovered as the first member of neurotrophin family, which promotes neural growth and includes some other factors, such as brain-derived neurotrophic factor, neurotrophin-3, and neurotrophin-4.^{3,4} Studies have proved the crucial regulatory and neurotrophic function of NGF during neu-

ral development, differentiation, and maturation. NGF also has a broad spectrum of protective effects on various neurons, glial cells, and vascular endothelial cells under different pathological circumstances.^{3,4} Further experiments demonstrate that the administration of NGF can reduce apoptotic cell death and infarct volume,^{5–8} ameliorate delayed neuronal death,⁹ steer microglia into neuroprotective phenotype,¹⁰ boost angiogenesis,¹¹ and promote neural regeneration and functional recovery.¹²

In the context of acute cerebral ischemia, the endogenous expression of NGF decreased significantly in infarcted cortex, highlighting the importance to deliver exogenous NGF.¹³ To this end, recombinant human NGF has been developed. There were a series of NGF clinical applications for traumatic and hypoxic-ischemic brain injury.^{14–16} However, the elimination half-life of NGF following intravenous injection is 2.3 h and 4.5 h via subcutaneous injection.¹⁷ For years, all these clinical attempts have shown that fast enzymatic degradation and poor permeability of the blood-brain barrier (BBB) make it challenging to deliver NGF into the central nervous system (CNS).¹⁸ It is thus of paramount importance to develop a novel strategy for the delivery of NGF into the brain efficiently and effectively.

Recently, increasing evidence has demonstrated that exosomes, 30- to 150-nm diameter extracellular vesicles, have emerged as promising drug carriers.¹⁹ Our previous work fused rabies virus glycoprotein (RVG) with exosomal protein lysosome-associated membrane glycoprotein 2b (Lamp2b). RVG-Lamp2b-modified exosomes can efficiently deliver microRNA-124 into brain.²⁰ It is important to develop

Received 23 February 2020; accepted 15 June 2020;
<https://doi.org/10.1016/j.omtn.2020.06.013>.

⁵These authors contributed equally to this work.

Correspondence: Guodong Yang, Department of Biochemistry and Molecular Biology, Fourth Military Medical University, No. 169 Changlexi Road, Xi'an, Shaanxi 710032, China.

E-mail: yanggd@fmmu.edu.cn

Correspondence: Yongjun Wang, China National Clinical Research Center for Neurological Diseases, Beijing, China; Department of Neurology, Beijing Tiantan Hospital, Capital Medical University, No. 119 Southwest of the Fourth Ring Road, Beijing 100070, China.

E-mail: yongjunwang@nccnd.org.cn



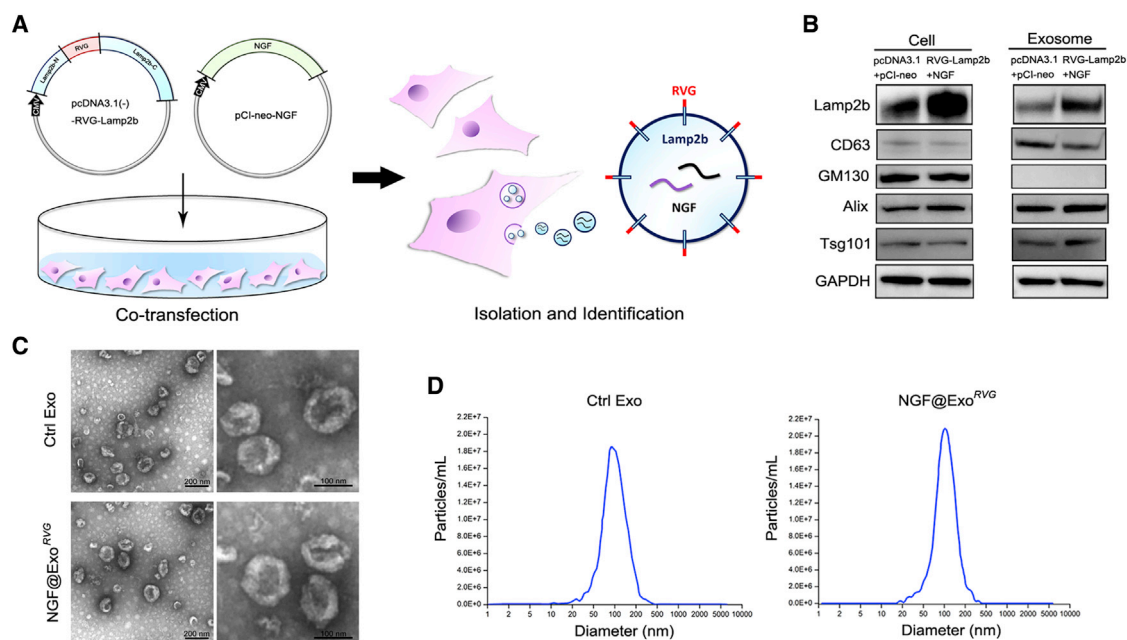


Figure 1. Construction and Characterization of NGF@Exo^{RVG}

(A) Schematic diagram of plasmid recombination, co-transfection, exosome isolation, and identification. HEK293 cells were co-transfected with pcDNA3.1(-)-RVG-Lamp2b and pCI-neo-NGF plasmids. The supernatant of cell culture was collected and went through ultracentrifugation to isolate NGF@Exo^{RVG}. (B) Western blot of Lamp2b, CD63, GM130, Alix, and Tsg101 in exosomes and parental cells transfected with pcDNA3.1(-) and pCI-neo plasmids (pcDNA3.1+pCI-neo) or pcDNA3.1(-)-RVG-Lamp2b and pCI-neo-NGF plasmids (RVG-Lamp2b+NGF). Note the increased expression of Lamp2b in modified cells and exosomes. (C) Representative electron microscopic images of Ctrl Exo and NGF@Exo^{RVG}. Scale bar, 100 nm or 200 nm, respectively. (D) Size distribution and concentration of Ctrl Exo and NGF@Exo^{RVG} analyzed by Zetaview.

a strategy to encapsulate larger mRNA and protein with more potent therapeutic effects via exosomes. In this study, we investigated whether recombinant human NGF protein and its mRNA could be loaded into RVG-Lamp2b-engineered exosomes, delivered into ischemic region, and translated directly in the recipient cells to reduce ischemic injury. We further examined the storage stability of modified exosomes and its therapeutic effects. Our study has established a novel and facile neurotrophin delivery strategy, which sheds light on the possible clinical application for stroke and some other CNS diseases in the future.

RESULTS

Construction and Characterization of NGF@Exo^{RVG}

To produce NGF@Exo^{RVG}, two recombinant vectors, namely pcDNA3.1(-)-RVG-Lamp2b and pCI-neo-NGF, were constructed. Both vectors were co-transfected into human embryonic kidney (HEK) 293 cells. The secreted exosomes from the transfected cells were isolated by sequential ultracentrifugation (Figure 1A), with the exosomes denoted as NGF@Exo^{RVG}.

As expected, RVG-Lamp2b fusion protein was overexpressed in cells transfected with RVG-Lamp2b and NGF vectors (RVG-Lamp2b+NGF), compared with control cells transfected with empty vectors pcDNA3.1(-) and pCI-neo (pcDNA3.1+pCI-neo). Consistently, RVG-Lamp2b was found in NGF@Exo^{RVG}, as shown by the more abundant Lamp2b bands (Figure 1B). Exosomal markers

CD63, Alix, and Tsg101 were highly expressed in both control exosomes (Ctrl Exo) and NGF@Exo^{RVG}, while Golgi marker GM130 was rarely detectable. The representative images of transmission electron microscopy (TEM) (Figure 1C) and nanoparticle tracking analysis (NTA) by Zetaview (Figure 1D) further showed that the modification of exosomes did not influence morphology, size, and production. Moreover, the production of exosomes was stable and repeatable. The yield of Ctrl Exo and NGF@Exo^{RVG} were $(2.78 \pm 0.05) \times 10^{11}$ particles and $(2.70 \pm 0.04) \times 10^{11}$ particles per microliter culture medium, respectively. It is important to note that the exosomes we claimed here should be “small extracellular vesicles” for accuracy according to the nomenclature endorsed by the International Society for Extracellular Vesicles.²¹

Efficient Loading of NGF into NGF@Exo^{RVG}

In order to explore whether NGF mRNA was encapsulated into the exosomes, a qRT-PCR assay was included. Exosomes were washed three times and purified again by ultracentrifugation before qRT-PCR. The results showed significantly increased levels of NGF mRNA in RVG-Lamp2b+NGF cells compared with pcDNA3.1+pCI-neo cells and untransfected ones (Figure 2A). Moreover, qRT-PCR revealed that there was a remarkable encapsulation of NGF mRNA into NGF@Exo^{RVG} (Figure 2B). Absolute qPCR revealed that approximately $0.87\% \pm 0.11\%$ of total RNA in NGF@Exo^{RVG} was NGF. A previous study has revealed that the mRNA in exosomes was approximately 8% of the mRNA detected in the donor cells,²²

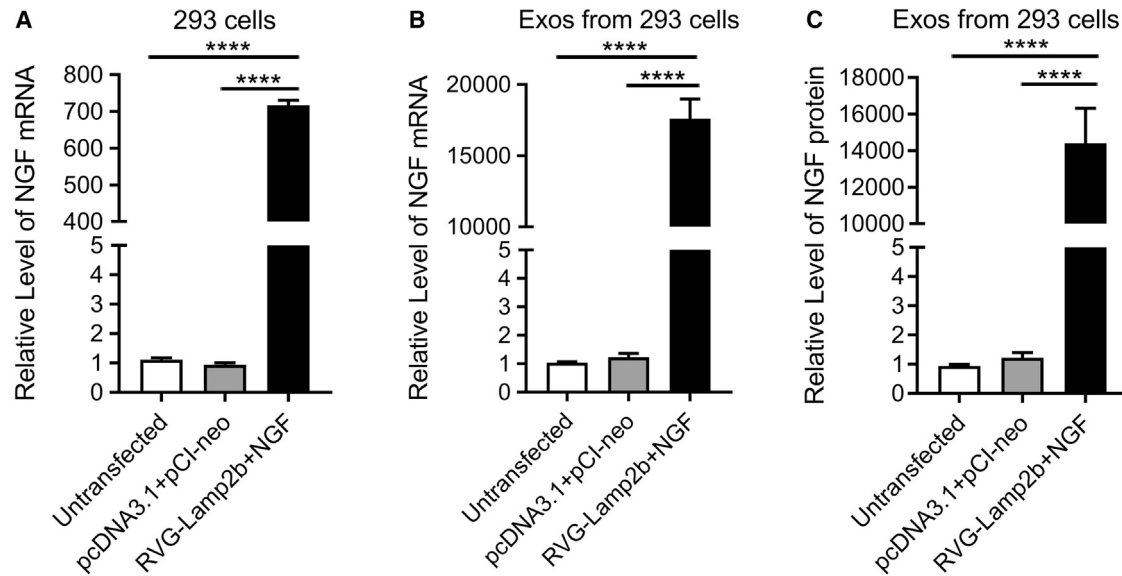


Figure 2. Efficient Loading of NGF into NGF@Exo^{RVG}

(A) The level of NGF mRNA in untransfected HEK293 cells and cells transfected with pcDNA3.1+pCI-neo or RVG-Lamp2b+NGF. (B) The level of NGF mRNA in exosomes derived from HEK293 cells treated as indicated. (C) The level of NGF protein in exosomes derived from HEK293 cells treated as indicated. Note the significant increase of NGF mRNA and protein in NGF@Exo^{RVG}. Data are presented as mean \pm SEM of three different experiments. **** $p < 0.0001$.

suggesting that the observed NGF abundance was relatively high and reasonable.

We further examined whether these exosomes could also carry NGF protein. Exosomes were washed and resuspended in PBS twice to wash away free NGF protein in cell culture supernatant. After wash and another round of ultracentrifugation, exosomes were lysed in RIPA and tested by using a human beta-NGF ELISA kit. The results showed that there was abundant NGF protein in NGF@Exo^{RVG}, while only marginal levels of NGF could be seen in Ctrl Exo and exosomes from untransfected cells (Figure 2C). Notably, there was about 31.37 ± 2.41 ng NGF protein per 100 μ g NGF@Exo^{RVG}. In other words, about $0.031\% \pm 0.002\%$ of the protein was NGF in NGF@Exo^{RVG}. The low abundance could be explained by the fact that NGF is a molecule with low molecular weight while most of the essential protein components of exosomes have large molecular weights. As to the mechanism of how NGF protein was encapsulated into the exosomes, we prefer the idea that the abundant expressed NGF protein in the donor cell was passively loaded into the exosomes, though potential active selection of NGF protein into the exosomes could not be excluded. Anyway, all these data showed that NGF mRNA and protein were encapsulated into NGF@Exo^{RVG} efficiently.

NGF@Exo^{RVG} Effectively Delivers NGF into Recipient Cells

Based on our findings that NGF@Exo^{RVG} could encapsulate abundant NGF mRNA and protein, we explored whether NGF@Exo^{RVG} could deliver NGF when exosomes were endocytosed by recipient cells. To this end, HEK293 cells were incubated with 0 μ g, 20 μ g, 50 μ g, 100 μ g, 200 μ g, or 300 μ g NGF@Exo^{RVG} for 4 h (Figure 3A). The amount of NGF mRNA increased most in 100 μ g group. There

was a relatively low level of NGF mRNA in recipient cells when incubated with 200 μ g or 300 μ g NGF@Exo^{RVG}, which might be explained by the saturation of endocytosis ability and unexpected toxicity caused by excessive exosomes (Figure 3B).

To investigate whether the delivered NGF mRNA could be translated into protein in recipient cells, we incubated HEK293 cells with 100 μ g NGF@Exo^{RVG}. After 4 h incubation, the medium was replaced with fresh growth medium and cultured for additional 2 h, 4 h, 8 h, 12 h, and 24 h. The NGF expression peaked at 271.46 ± 21.47 pg per 1 mg cell lysate at 8 h, followed by a slow drop from 12 to 24 h (Figure 3C), which might be due to the degradation of delivered NGF protein. To further confirm the translation of delivered NGF mRNA into protein, we pretreated HEK293 cells with 10 μ g/mL cycloheximide (CHX) for 2 h, a known translation inhibitor. Compared with the group with no CHX pretreatment, there was a significant decrease of NGF protein in HEK293 cells treated with CHX (Figure S1). Thus, though the absolute level of NGF mRNA in exosomes was low, it produced robust protein in the recipient cells. Our findings were consistent with those of previous studies that exosomal mRNA is functional when delivered into recipient cells.^{23–25} These results demonstrated that NGF@Exo^{RVG} could effectively deliver NGF mRNA and protein into recipient cells.

NGF@Exo^{RVG} Retains Stability after Longtime Storage

Aimed for future clinical application, the stability of NGF@Exo^{RVG} after longtime storage is of crucial importance. After sequential centrifugation, NGF@Exo^{RVG} was stored at -80°C from 1 month to 3 months. Compared with the exosomes derived from

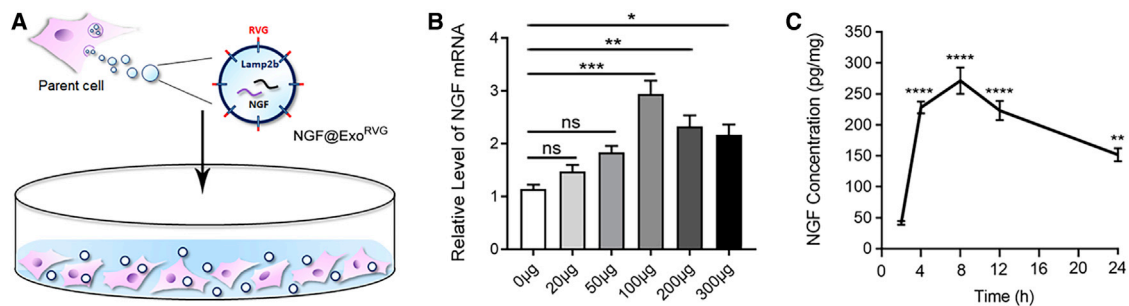


Figure 3. NGF@Exo^{RVG} Effectively Delivers NGF into Recipient Cells

(A) Schematic diagram of the treatment of HEK293 cells with NGF@Exo^{RVG}. (B) The level of NGF mRNA in HEK293 cells treated with different dosages of NGF@Exo^{RVG}. HEK293 cells were harvested at 4 h. Note the highest level of NGF mRNA in cells treated with 100 μ g NGF@Exo^{RVG}. (C) The level of NGF protein in HEK293 cells treated with 100 μ g NGF@Exo^{RVG}. HEK293 cells were harvested at 2 h, 4 h, 8 h, 12 h, and 24 h as indicated. Data are presented as mean \pm SEM of three different experiments. * p < 0.05; ** p < 0.01; *** p < 0.001; **** p < 0.0001. ns = no significance.

untransfected HEK293 cells, there was a significant increase of NGF mRNA level in freshly harvested and 1-month- or 3-month-stored NGF@Exo^{RVG}. The level was not affected significantly by low temperature storage between the latter three groups (Figure 4A), indicating the stability of encapsulated mRNA in NGF@Exo^{RVG}. Then, we incubated 100 μ g freshly harvested NGF@Exo^{RVG}, 1-month- or 3-month-stored NGF@Exo^{RVG} with HEK293 cells and examined the level of NGF mRNA and protein in recipient cells. Similarly, the longtime storage did not influence the delivery of NGF mRNA and the efficiency of the following translation in acceptor cells (Figures 4B and 4C). All these results showed that NGF@Exo^{RVG} retained stability after longtime storage at -80°C , endowing NGF@Exo^{RVG} with the potential as an off-the-shelf therapeutic drug for clinical application.

NGF@Exo^{RVG} Effectively Delivers NGF into Ischemic Region

To explore the efficacy of NGF@Exo^{RVG} transporting NGF to the ischemic region, we developed a photothrombotic ischemia model as previously described.²⁰ Exosomes were injected in the tail vein 24 h post-ischemia. Mice were sacrificed at 2 h for fluorescent exosome tracking, 4 h for qRT-PCR analysis, and 8 h for NGF ELISA analysis (Figure 5A).

To visualize the *in vivo* distribution, 200- μ g exosomes in 200 μ L saline were labeled with 1,1'-dioctadecyl-3,3,3',3'-tetramethylindocarbocyanine perchlorate (DiI) dye. Few DiI signals could be observed in the infarcted cortex in mice injected with Ctrl Exo. However, remarkable DiI-positive ischemic region could be detected in Exo^{RVG}- and NGF@Exo^{RVG}-injected mice (Figure 5B). Similar with our previous findings,²⁰ the diffuse DiI signals in the ischemic area overlapped with the markers of neurons, microglia, and astrocytes, suggesting that the exosomes could be uptaken by these cell types (Figure S2). Consistent with the published study,²⁶ robust DiI signals were observed in reticuloendothelial system, such as liver, spleen, and lung. Notably, slightly weaker fluorescent signals in these organs could be seen in Exo^{RVG} and NGF@Exo^{RVG} groups (Figure 5B). All these indicated that RVG-Lamp2b modification could steer more exosomes into ischemic region.

In the following experiments, we explored whether NGF@Exo^{RVG} could deliver NGF mRNA and protein into the ischemic region. We compared the level of delivered NGF mRNA in the contralateral and ipsilateral ischemic cortex in Ctrl Exo-, NGF@Exo^{ctrl}-, and NGF@Exo^{RVG}-injected mice. Treatment of NGF@Exo^{RVG} remarkably increased the level of NGF mRNA in ipsilateral cortex. Notably, NGF@Exo^{ctrl} delivered NGF mRNA at a much lower level than that of NGF@Exo^{RVG} group (Figure 5C; Figure S3A). Consistently, ELISA assay at 8 h post-treatment showed the highest level of NGF protein in NGF@Exo^{RVG}-treated mice (Figure 5D; Figure S3B). Previous study has reported that most exosomes that penetrated the mouse brain are located in the parenchyma rather than in the circulation at 24 h post-intravenous injection.²⁷ To confirm that the detected NGF mRNA and protein were intracellular rather than free exosomes, we then examined the level of NGF mRNA and protein 24 h after in tail-vein injection. Consistent with the data examined at earlier time points (qRT-PCR at 4 h and ELISA at 8 h), there remained a significantly higher level of NGF mRNA and protein in ischemic region in mice with NGF@Exo^{RVG} treatment (Figure S4). Collectively, these data demonstrated that NGF@Exo^{RVG} could efficiently deliver NGF into ischemic cortex.

NGF@Exo^{RVG} Reduces Ischemic Injury via Reducing Inflammation and Cell Death

NGF has multifaceted neuroprotective functions in pathological processes, such as promotion of cell survival and neurogenesis, anti-apoptosis, and anti-inflammation. To investigate the effects of NGF on cortical ischemia, we injected 200 μ L saline, 200 μ g Ctrl Exo, Exo^{RVG} or NGF@Exo^{RVG} in 200 μ L saline only once at 1 day post-ischemia (dpi). Mice were sacrificed at 7 dpi, and brain cryostat sections were made for immunostaining. Previous studies have highlighted the importance of microglia polarization in brain injury and repair. Classically activated (M1) microglia release proinflammatory factors and induces oxidative stress. By contrast, alternatively activated (M2) microglia promote restorative processes such as neurogenesis, axonal regeneration, and remyelination.²⁸ Since NGF has been proved its ability to steer microglia toward a neuroprotective

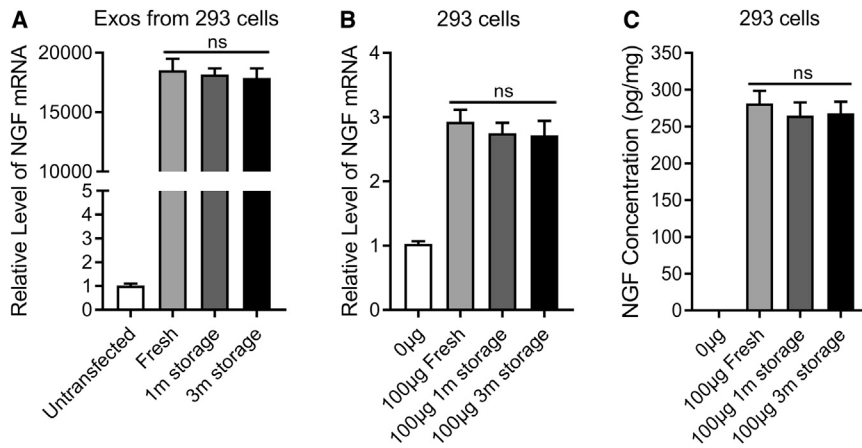


Figure 4. Stability of NGF@Exo^{RVG}

(A) The level of NGF mRNA in exosomes from the following samples: exosomes freshly harvested from untransfected HEK293 cells, freshly harvested NGF@Exo^{RVG}, and 1-month (1 m)- and 3-month (3 m)-stored NGF@Exo^{RVG}. (B) The level of NGF mRNA in HEK293 cells treated with 100 µg freshly harvested NGF@Exo^{RVG} and 1 m- and 3 m-stored NGF@Exo^{RVG}. HEK293 cells were harvested at 4 h. (C) Expression of NGF protein in HEK293 cells treated with 100 µg freshly harvested NGF@Exo^{RVG} and 1 m- and 3 m-stored NGF@Exo^{RVG}. HEK293 cells were harvested at 8 h. The bar was not visible in 0-µg group as the levels were below the detection limit. Note there was no significant difference between groups of freshly harvested and longtime-stored NGF@Exo^{RVG}. Data are presented as mean ± SEM of three different experiments. ns = no significance.

phenotype,¹⁰ we examined the expression of microglia marker Iba1, CD16 (M1 type), and CD206 (M2 type) in the ischemic region to explore whether a single injection of NGF@Exo^{RVG} could bias microglia polarization into protective M2 type. Non-specific control with secondary antibody only was applied to ensure the specific staining following identical procedures and microscope settings (Figure 6A). In the saline, Ctrl Exo, and Exo^{RVG} groups, Iba1-positive microglia exhibited amoeboid shape with scarce dendrites, in contrast to the ramified morphology with elongated dendrites in sham-operated controls (Figure 6B). The double staining of CD16/Iba1 and CD206/Iba1 demonstrated approximately 72.3%, 70.6%, and 68.7% CD16⁺ M1 microglia, 26.5%, 28.0%, and 27.5% CD206⁺ M2 microglia in saline, Ctrl Exo, and Exo^{RVG} groups, respectively (Figures 6C and 6D). Notably, the treatment of NGF@Exo^{RVG} significantly reduced the percentage of CD16⁺ M1 microglia to 39.4%, while increasing the proportion of CD206⁺ M2 microglia to approximately 67.5% in ischemic cortex. Interestingly, we did not observe significant decrease of Iba1-positive cells (data not shown). These results verified that NGF@Exo^{RVG} could promote the polarization of neuroprotective M2 phenotype after ischemia.

It has been proved that NGF administration can ameliorate apoptotic cell death after ischemia. TUNEL staining was performed to assay cell death at 7 dpi (Figure 7A). Fluorescence images and cell quantification in the ischemic region showed that TUNEL-positive cells were significantly reduced in NGF@Exo^{RVG}-treated mice compared with the saline, Ctrl Exo, and Exo^{RVG} group (Figure 7B). These confirmed that NGF@Exo^{RVG} treatment could promote cell survival.

In view of the above data concerning the multiple protective effects of NGF@Exo^{RVG} on anti-inflammation and pro-survival, we asked whether NGF@Exo^{RVG} could promote neurogenesis post-ischemia. In saline, Ctrl Exo, and Exo^{RVG} groups, few doublecortin (DCX)-labeled cells scattered around the infarcted region. However, the number of DCX-positive cells in NGF@Exo^{RVG}-treated mice approximately tripled that in control ones (Figures 8A and 8B), suggesting possible neurogenesis post ischemia.

DISCUSSION

In this study, we loaded RVG-Lamp2b exosomes with NGF to generate NGF@Exo^{RVG}. One injection of NGF@Exo^{RVG} efficiently delivered NGF into ischemic cortex and thus ameliorated inflammation, reduced cell death, and promoted DCX-positive cells. To our knowledge, this is the first study that delivers NGF mRNA and protein via engineered exosomes into infarcted region with promising therapeutic effects.

NGF is one of the most well-known neurotrophic factors with remarkable potential in the treatment for CNS diseases. In CNS, neurons, astrocytes, and microglia can produce NGF and also react to it. NGF exhibits a variety of protective abilities including reducing apoptosis, promoting cell survival, and neural regeneration in pathological settings.³ In our study, exosomal delivery of NGF significantly modulates M2 microglial polarization, promotes cell resistance to death, and possibly boosts neurogenesis in ischemic region, directly confirming the potential of NGF@Exo^{RVG} therapy for cerebral ischemia. And it is thus interesting to investigate whether NGF@Exo^{RVG} treatment can promote functional recovery by behavioral tests in future study.

Delivery of therapeutic drugs bypassing BBB has long been a challenging question. Virus vector, NGF gene manipulated cells, nano capsules, and hydrogels have already been used as NGF transporting vehicles.^{29–32} However, these attempts have failed to deliver NGF to targeted brain parenchyma via systemic administration. Short *in vivo* half-life, poor pharmacokinetic profile, failure to cross the BBB, and unwanted pleiotropic effects in peripheral tissues due to nonspecific uptake hinder NGF from clinical application for brain disorders.^{33–35}

Recently, studies report that exosomes are of great drug delivery value due to their high physicochemical stability and biocompatibility with low toxicity and immunogenicity. Its ability to transfer nucleic acids and proteins from parent cells to acceptor cells, thereby triggering phenotypic changes in the latter, has generated extensive interest in exosome-based therapy.³⁶ The amenability of

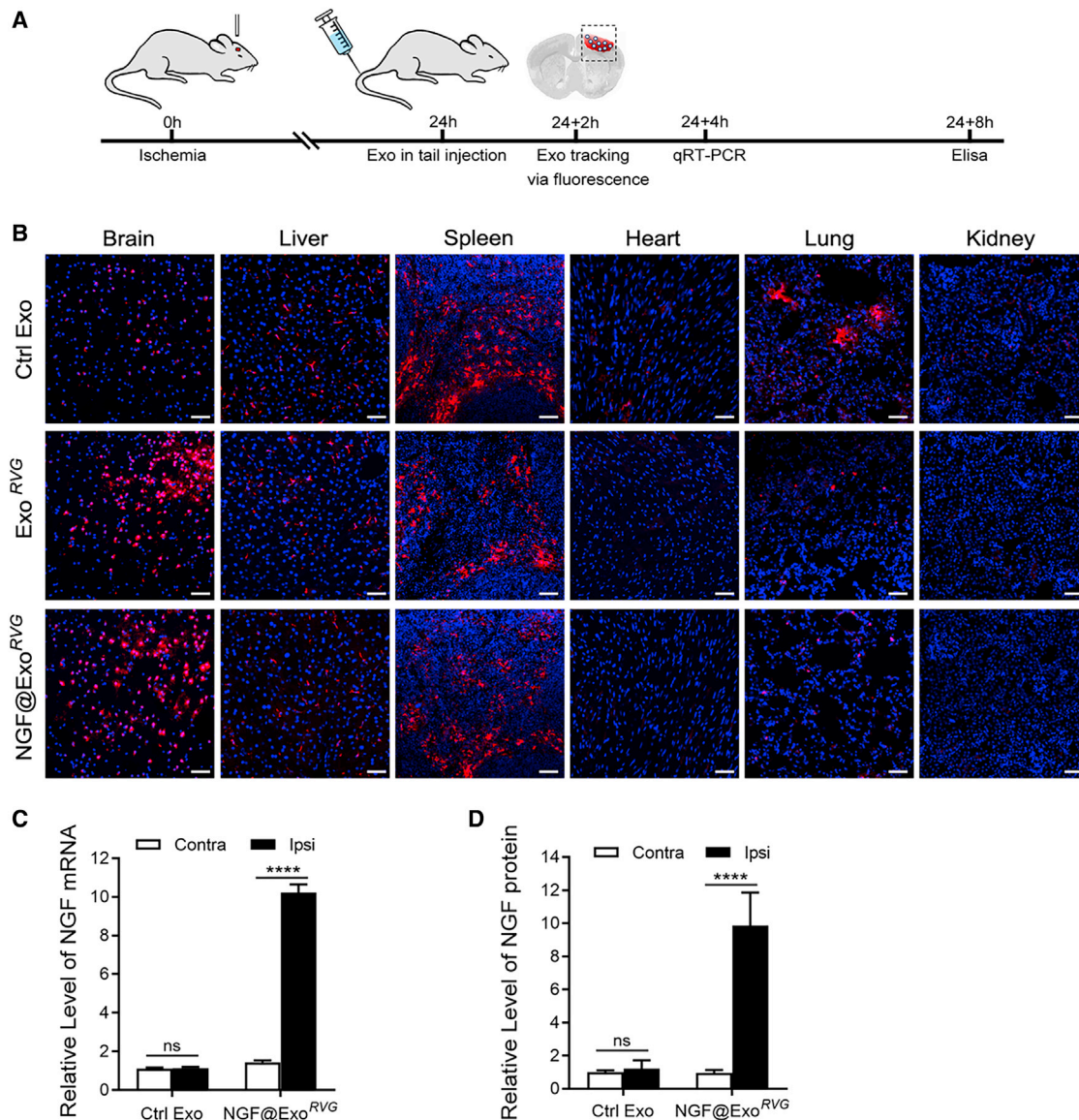


Figure 5. NGF@Exo^{RVG} Effectively Delivers NGF into Ischemic Region

(A) Schematic diagram of experimental procedure. (B) *In vivo* tracking of 200 μ g Dil-labeled Ctrl Exo, Exo^{RVG}, and NGF@Exo^{RVG}. Brain, liver, spleen, heart, lung, and kidney were harvested 2 h post in tail-vein injection of exosomes, and then frozen sections were made. Rare Dil labeling signals observed in ischemic region in Ctrl Exo group, in contrast to the remarkable Dil labeling in Exo^{RVG} and NGF@Exo^{RVG} group. Scale bar, 50 μ m. (C and D) The level of NGF mRNA (C) and protein (D) in contralateral (Contra) and ipsilateral (Ipsi) cortex in Ctrl Exo- and NGF@Exo^{RVG}-treated mice. Note the remarkable increase of NGF mRNA and protein in ischemic cortex. Data are presented as mean \pm SEM of five mice. **** $p < 0.0001$. ns = no significance.

membrane modification and intrinsic ability of traversing the BBB further facilitate the targeted drug transport to the brain.³⁷ As for neurotrophins, which need post-translational modification in cytoplasm and are secreted to exert their biological functions in a paracrine manner, the delivery of mRNA may be a more efficient and safer approach for protein substitution in targeted cells.³⁸ Unlike plasmid DNAs and viral vectors, mRNAs do not integrate with the genome and therefore pose no risk of insertional mutagenesis. However, the direct application of naked mRNAs has to face the ob-

stacles such as the rapid extracellular degradation by ubiquitous RNases, hampered passive diffusion by cell membrane, and limited cell uptake capacity.³⁹ Exosome-mediated mRNA delivery provides a novel strategy to overcoming these obstacles to supplement proteins in the targeted region. Previous studies and our group's work have shown that RVG-modified exosomes can deliver small interfering RNA (siRNA) and microRNA (miRNA) into the brain.^{20,40} In this study, NGF mRNA was loaded into RVG-modified exosomes, delivered into ischemic cortex, and translated into

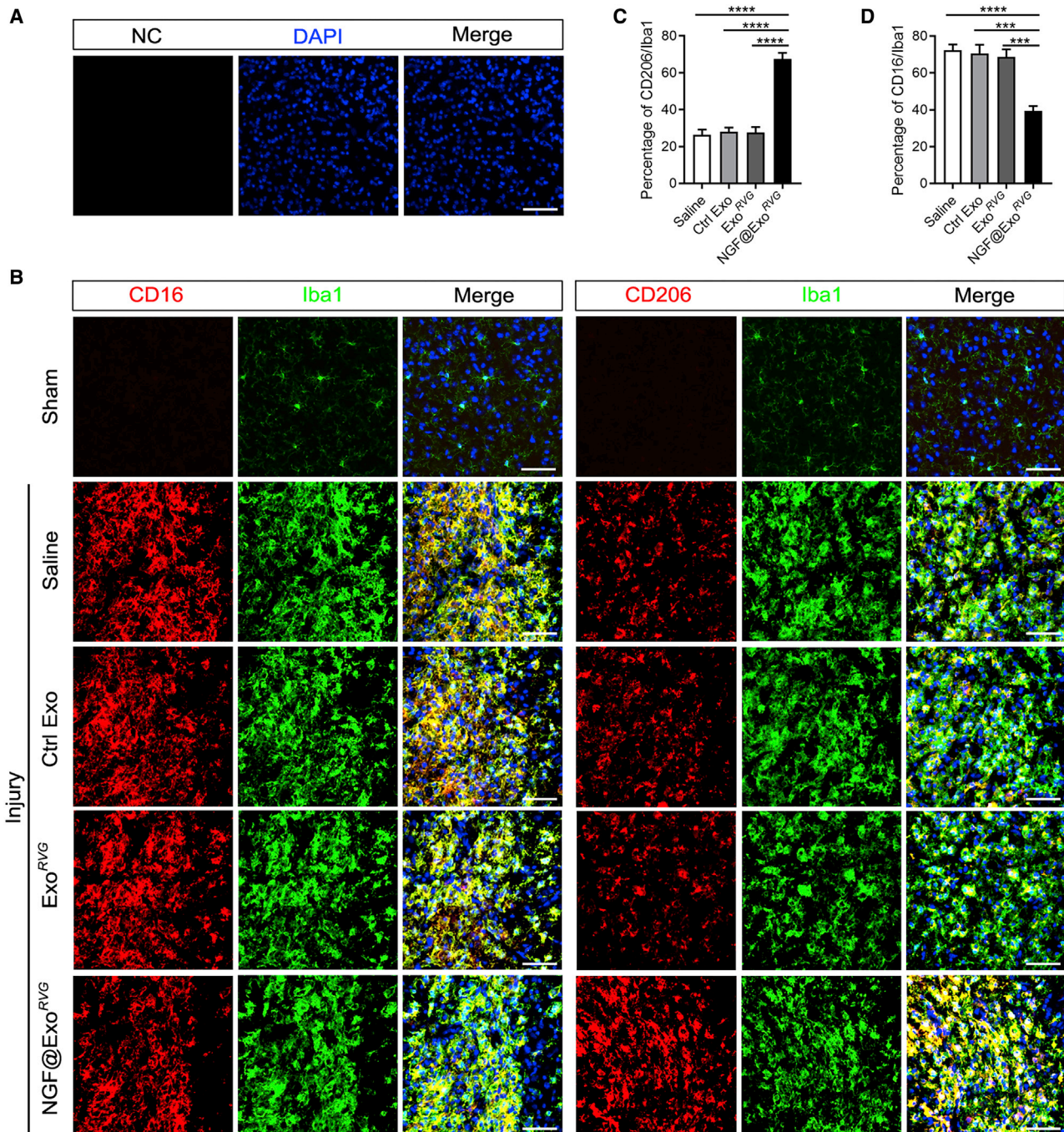


Figure 6. Effects of NGF@Exo^{RVG} on Microglia Polarization in Ischemic Region

(A) Immunofluorescence images of secondary antibody negative control (NC) to confirm the specificity of the immunostaining. (B) Representative immunofluorescence images of CD16, CD206, and Iba1 staining in the ischemic cortex of sham group and saline-, Ctrl Exo-, Exo^{RVG}-, and NGF@Exo^{RVG}-treated groups at 7 dpi. Note the significant decreased expression of CD16 and increased expression of CD206 in NGF@Exo^{RVG}-treated mice compared with sham, saline-, Ctrl Exo-, and Exo^{RVG}-treated groups. (C and D) Cell quantification of the percentage of CD206/Iba1 (C) and CD16/Iba1 (D) in the ischemic region. Scale bar, 50 μ m. Data are presented as mean \pm SEM of five mice. *** p < 0.001; **** p < 0.0001.

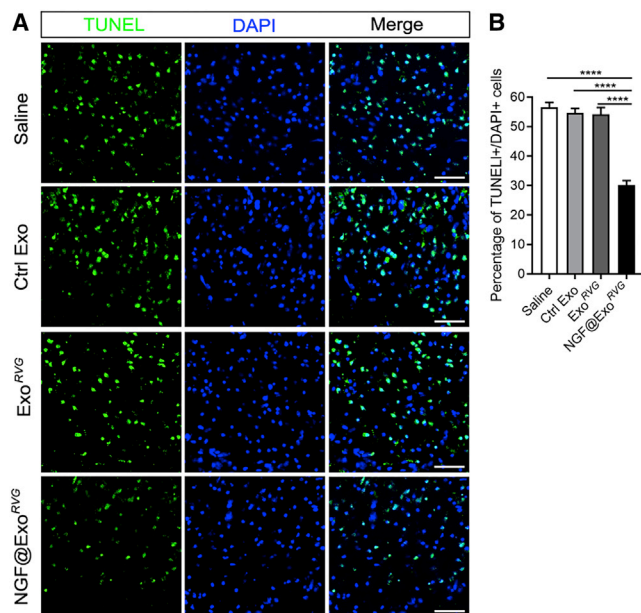


Figure 7. Effects of NGF@Exo^{RVG} on Cell Apoptosis in Ischemic Region

(A) Representative immunofluorescence images of TUNEL staining in the ischemic cortex of saline-, Ctrl Exo-, Exo^{RVG}-, and NGF@Exo^{RVG}-treated mice at 7 dpi. Note the significant decreased expression of TUNEL in NGF@Exo^{RVG}-treated mice. (B) Cell quantification of the percentage of TUNEL-positive/DAPI-positive cells in the ischemic region. Scale bar, 50 μ m. Data are presented as mean \pm SEM of five mice. **** p < 0.0001.

bioactive NGF protein in recipient cells. Our strategy significantly increased the expression of NGF mRNA and NGF protein in infarcted cortex, where endogenous NGF was barely detected at 1 dpi.¹³ An amount of NGF protein was also encapsulated into NGF@Exo^{RVG}. This may provide a burst release of pioneering NGF protein for immediate rescue, facilitating further NGF mRNA translation in injured cells. *In vivo* DiI tracking showed the steered distribution of NGF@Exo^{RVG} to ischemic cortex from other main organs, suggesting that there will be less toxicity and pleiotropic effects when applied systemically. Additionally, only a single injection of 200 μ g NGF@Exo^{RVG} at 1 dpi was carried out in our study, indicating high delivery efficiency and long-lasting therapeutic effects. The proposed strategy thus might have some advantages over the repetitive injections of NGF protein intravenously or subcutaneously in future clinical therapy, which would be worth further study by direct comparison.

For the first time, we found that NGF@Exo^{RVG} remain stable after longtime storage. Several clinical studies have used exosomes stored at -80°C .⁴¹ It would be interesting to test the stability of exosomes stored at higher temperatures or in lyophilized and reconstituted condition for easy storage and transportation. There also remain challenges for clinical application of exosome-mediated neurotrophin delivery. For example, optimization of mRNA loading, clinical-grade purification, and large-scale production of exosomes with high yields are needed for clinical use in the future.

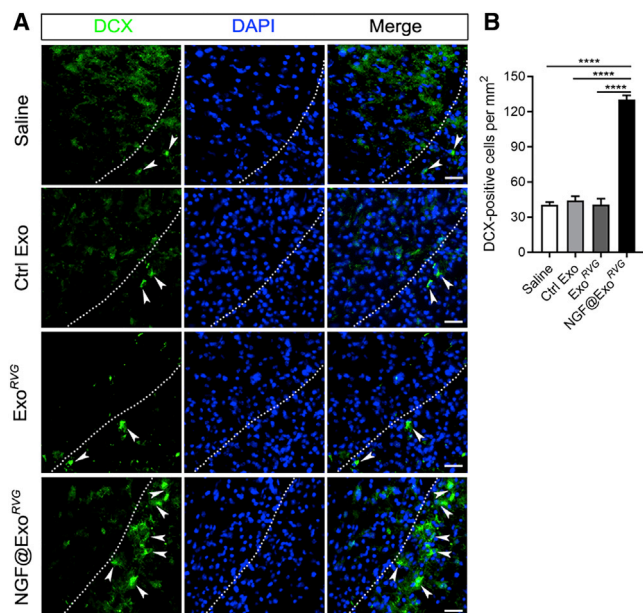


Figure 8. NGF@Exo^{RVG} Promotes Neurogenesis Effectively in Ischemic Region

(A) Representative immunofluorescence images of DCX staining in the ischemic cortex of saline-, Ctrl Exo-, Exo^{RVG}-, and NGF@Exo^{RVG}-treated mice at 7 dpi. Note the significant increased expression of DCX in NGF@Exo^{RVG}-treated mice. (B) Cell quantification of the number of DCX-positive cells per mm² ischemic region. Scale bar, 25 μ m. Data are presented as mean \pm SEM of five mice. **** p < 0.0001.

Conclusion

In conclusion, our findings highlight the potential therapeutic effects of targeted exosome-delivered NGF in ischemic cortex. The strategy proposed in our preclinical study shows great promise for future stroke therapy.

MATERIALS AND METHODS

Animals and Photothrombosis Model

C56BL/6 mice (male, 8–9 weeks old, 22–23 g) were used. All animal experiments were carried out under protocols approved by the Animal Care and Use Committee of the Beijing Institute of Biotechnology. Focal cortical ischemia was made as previously described.²⁰ In brief, after the tail-vein injection of rose bengal (Sigma-Aldrich, St. Louis, MO, USA) at 25 mg/kg, the skull window ranging from 0.5 to 2.5 mm posterior to the bregma and 0.5 to 2.5 mm right to the midline was illuminated for 8 min by an optic fiber connected to a 532-nm light source. Sham-operated mice underwent the same procedures, except for the light illumination. To investigate the effects of exosomes *in vivo*, 200 μ g Ctrl Exo, Exo^{RVG}, NGF@Exo^{Ctrl}, or NGF@Exo^{RVG} in 200 μ L saline were injected into the tail vein only once at 1 dpi.

Cell Culture

HEK293 cells, obtained from National Infrastructure of Cell Line Resource (Beijing, China), were cultured in Dulbecco's Modified

Eagle's Medium (DMEM; Gibco, Grand Island, NY, USA) supplemented with 10% fetal bovine serum (FBS; Gibco, Grand Island, NY, USA) and 1% penicillin-streptomycin (Gibco, Grand Island, NY, USA) at 37°C, 5% CO₂.

Exosome Engineering

Lamp2b was cloned with cDNA from mouse cortex and was inserted between NheI and BamHI into a pcDNA3.1(-) vector as previously described.²⁰ Primers designed to encode RVG were used to introduce the targeting ligand between XhoI and BspEI. The gene of human beta-NGF with three amino acids removed from the C terminus was synthesized and inserted between EcoRI and NotI into a pCI-neo vector as previously described.³¹ One hour before transfection, the cell culture medium was changed into DMEM, without FBS or antibiotics. To produce NGF@Exo^{RVG}, HEK293 cells were transfected with pcDNA3.1(-)-RVG-Lamp2b and pCI-neo-NGF plasmids by TurboFect transfection reagent (Thermo Fisher Scientific, Waltham, MA, USA). Cells transfected with pcDNA3.1(-) and pCI-neo plasmids were used to produce Ctrl Exo. Cells transfected with pcDNA3.1(-)-RVG-Lamp2b and pCI-neo plasmids were used to produce Exo^{RVG}, and cells transfected with pcDNA3.1(-) and pCI-neo-NGF plasmids were used for production of NGF@Exo^{Ctrl}. Six hours after transfection, cell culture medium was changed into DMEM with 10% exosome-depleted FBS. To obtain exosome-free FBS, FBS was ultracentrifuged at 100,000 × *g* for 2 h at 4°C as previously described.⁴² Transfected cells were cultured for 48 h and prepared for exosome isolation.

Exosome Isolation and Characterization

Exosomes were purified from cell culture supernatant of HEK293 cells. Prior to culture medium collection, HEK293 cells were washed twice with PBS and were cultured in the medium supplemented with 10% exosome-depleted FBS. After incubation for 48 h, the supernatant was collected and went through sequential ultracentrifugation at 2,000 × *g* for 30 min, 10,000 × *g* for 30 min, and 100,000 × *g* for 2 h at 4°C. The exosomes were washed with PBS and resuspended for further characterization.

For *in vivo* fluorescence labeling of exosomes, a 2-mg/mL solution of DiI (Solarbio Science & Technology, China) was added to the PBS (1:200) following the manufacturer's instructions. After the isolation by ultracentrifugation as mentioned above, DiI-labeled exosomes (DiI-Exos) were resuspended in 0.9% saline and centrifuged at 12,000 × *g* for 1 h. This procedure was repeated for three times to wash free DiI away. Then DiI-Exos were injected intravenously through the tail vein into ischemic mice at 1 dpi.

For TEM, 20-μL purified exosomes in sterile-filtered PBS was added onto a carbon-coated copper grid for 15 min. Afterward, the grid was stained with 2% uranyl acetate (UA) for 1 min. The excess UA was removed, and the grid was washed of distilled water. Then the grid was dried for 15 min and imaged by transmission electron microscope (JEM-2000EX, JEOL, Tokyo, Japan).

For NTA, Zetaview (ParticleMetrix, Germany) was used to analyze the size distribution and concentration of exosomes. Exosome samples were diluted at 1:1,000 for Zetaview analysis.

Western Blot

For cell and exosome western blot, samples were lysed by RIPA buffer (Thermo Fisher Scientific, Waltham, MA, USA). The amount of protein was determined using a bicinchoninic acid protein assay kit (Thermo Fisher Scientific, Waltham, MA, USA). After protein transfer, the polyvinylidene fluoride (PVDF) membranes were blocked with 5% Difco skim milk (BD Biosciences, San Diego, CA, USA) in Tris-buffered saline containing 0.1% Tween-20 (TBST) for 1 h. Blots were incubated with primary antibodies overnight at 4°C. The primary antibodies used were as follows: rabbit anti-CD63 (1:1,000, Abcam, cat. ab217345; Cambridge, MA, USA), rabbit anti-GM130 (1:1,000, Abcam, cat. ab52649; Cambridge, MA, USA), rabbit anti-Lamp2b (1:2,000, Abcam, cat. ab199946; Cambridge, MA, USA), mouse anti-Alix (1:1,000, Cell Signaling Technology, cat. 2171; Danvers, MA, USA), mouse anti-Tsg101 (1:1,000, Abcam, cat. ab83; Cambridge, MA, USA), rabbit anti-GAPDH (1:1,000, Cell Signaling Technology, cat. 2118; Danvers, MA, USA). Corresponding horseradish peroxidase (HRP)-conjugated anti-mouse or anti-rabbit immunoglobulin G (IgG) (1:10,000, Pierce, Rockford, IL, USA) secondary antibodies were incubated for 1 h at room temperature. Bands were detected using an enhanced chemiluminescence (ECL) kit (Pierce, Rockford, IL, USA).

RNA Isolation and qRT-PCR

Total RNA was extracted from cells, exosomes, or ipsilateral/contralateral cortex using RNAiso Plus (Takara, Tokyo, Japan) according to the manufacturer's instructions.

For analysis of mRNA levels, reverse transcription was performed using PrimeScript RT master mix (Takara, Tokyo, Japan), and cDNAs were used for qRT-PCR using TB green premix Ex Taq II (Takara, Tokyo, Japan). Primers for human NGF were as follows: forward, 5'-AGCGGCGATAGCTGCACGCGTGGCG-3'; reverse, 5'-CAGATCCTGAGTGTCTGCAGCTTAC-3'. Primers for human GAPDH were as follows: forward, 5'-GAAGGCTGGGGCTCATT-3'; reverse, 5'-CAGGAGGCATTGCTGATGAT-3'. Primers for mouse *Gapdh* were as follows: forward, 5'-GGTTGTCTCCTGC GACTTCA-3'; reverse, 5'-TGGTCCAGGGTTTCTTACTCC-3'. No reverse transcriptase control and no template control were included to confirm the quality of templates and primers, respectively. The qRT-PCR was performed in an Applied Biosystems ViiA 7 real-time PCR system, applying the following amplification parameters: 95°C for 30 s, followed by 40 cycles of 95°C for 5 s and 65°C for 34 s. All qRT-PCR reactions were run in triplicate, and mRNA expression relative to GAPDH was calculated using the 2^{-ΔΔCt} method.

Immunofluorescence and Image Analysis

Frozen serial sections of brain, liver, spleen, heart, lung, and kidney of 14 μm in thickness were prepared on cryostats. After incubation with 3% bovine serum albumin (BSA) and 0.3% Triton X-100 in

PBS for 1 h, the following primary antibodies were incubated overnight at room temperature: rabbit anti-Iba1 (1:1,000, cat. 019-19741, Wako, Japan), rat anti-CD16 (1:200, cat. 553142, BD Biosciences, San Jose, CA, USA), goat anti-CD206 (1:200, cat. AF2535, R&D Systems, Minneapolis, MN, USA), rabbit anti-DCX (1:500, cat. ab18723, Abcam, Cambridge, MA, USA). Corresponding secondary antibodies, namely Alexa Fluor 488 and Alexa Fluor 594 (donkey anti-rabbit, anti-rat, or anti-goat IgG, 1:500; Thermo Fisher Scientific, Waltham, MA, USA), were incubated for 2 h at room temperature. Secondary antibody negative controls were performed. Cell nuclei were stained by DAPI. TUNEL staining was performed according to the manual of DeadEND TUNEL system (Promega, Madison, WI, USA). The ischemic region was defined by the area enriched with nuclei in shrinkage and with disordered arrangement, which was apparently different from the normal adjacent area. Cells in the ischemic region were counted from every eighth slice. Five mice were included for each group. The percentage of CD16⁺ M1 microglia or CD206⁺ M2 microglia was calculated by the number of CD16⁺ cells/Iba1⁺ cells or CD206⁺ cells/Iba1⁺ cells. The percentage of TUNEL⁺ cells was calculated against DAPI⁺ nuclei. The percentage of DCX⁺ cells was calculated against the infarct area, while the infarct area was counted by ImageJ (National Institutes of Health, Bethesda, MD, USA). The quantitative analysis was performed in a design-blind way.

NGF ELISA

Human beta-NGF DuoSet ELISA (R&D Systems, Minneapolis, MN, USA) was used to detect the expression of NGF. The samples were lysed and measured with a standard curve established according to manufacturer's instructions.

Statistical Analysis

Data were presented as mean \pm SEM. Analyses were performed using GraphPad Prism v8.0. The significance of the differences was assessed by one-way analysis of variance (ANOVA) followed by Tukey's multiple comparison tests. $p < 0.05$ was considered as statistically significant.

SUPPLEMENTAL INFORMATION

Supplemental Information can be found online at <https://doi.org/10.1016/j.omtn.2020.06.013>.

AUTHOR CONTRIBUTIONS

Conceptualization, Methodology, and Writing, J.Y., G.Y., and Y.W.; Investigation, J.Y., S.W., and D.Z.; Resources, G.Y., Y.W., L.H., and S.Y.; Funding Acquisition, J.Y.

CONFLICTS OF INTEREST

The authors declare no competing interests.

ACKNOWLEDGMENTS

This work was supported by the National Natural Science Foundation of China (NSFC81801161) and the China Postdoctoral Science Foundation (2019M660722) to J.Y. The authors thank all the lab members

of Yang and Hou labs for technical support and critical discussion of the manuscript.

REFERENCES

- Collaborators, G.N.; GBD 2016 Neurology Collaborators (2019). Global, regional, and national burden of neurological disorders, 1990-2016: a systematic analysis for the Global Burden of Disease Study 2016. *Lancet Neurol.* 18, 459-480.
- Zerna, C., Thomalla, G., Campbell, B.C.V., Rha, J.H., and Hill, M.D. (2018). Current practice and future directions in the diagnosis and acute treatment of ischaemic stroke. *Lancet* 392, 1247-1256.
- Sofroniew, M.V., Howe, C.L., and Mobley, W.C. (2001). Nerve growth factor signaling, neuroprotection, and neural repair. *Annu. Rev. Neurosci.* 24, 1217-1281.
- Rocco, M.L., Soligo, M., Manni, L., and Aloe, L. (2018). Nerve Growth Factor: Early Studies and Recent Clinical Trials. *Curr. Neuropharmacol.* 16, 1455-1465.
- Holtzman, D.M., Sheldon, R.A., Jaffe, W., Cheng, Y., and Ferriero, D.M. (1996). Nerve growth factor protects the neonatal brain against hypoxic-ischemic injury. *Ann. Neurol.* 39, 114-122.
- Guégan, C., Onténiente, B., Makiura, Y., Merad-Boudia, M., Ceballos-Picot, I., and Sola, B. (1998). Reduction of cortical infarction and impairment of apoptosis in NGF-transgenic mice subjected to permanent focal ischemia. *Brain Res. Mol. Brain Res.* 55, 133-140.
- Saito, A., Narasimhan, P., Hayashi, T., Okuno, S., Ferrand-Drake, M., and Chan, P.H. (2004). Neuroprotective role of a proline-rich Akt substrate in apoptotic neuronal cell death after stroke: relationships with nerve growth factor. *J. Neurosci.* 24, 1584-1593.
- Cao, J.Y., Lin, Y., Han, Y.F., Ding, S.H., Fan, Y.L., Pan, Y.H., Zhao, B., Guo, Q.H., Sun, W.H., Wan, J.Q., and Tong, X.P. (2018). Expression of nerve growth factor carried by pseudotyped lentivirus improves neuron survival and cognitive functional recovery of post-ischemia in rats. *CNS Neurosci. Ther.* 24, 508-518.
- Shigeno, T., Mima, T., Takakura, K., Graham, D.I., Kato, G., Hashimoto, Y., and Furukawa, S. (1991). Amelioration of delayed neuronal death in the hippocampus by nerve growth factor. *J. Neurosci.* 11, 2914-2919.
- Rizzi, C., Tiberi, A., Giustizieri, M., Marrone, M.C., Gobbo, F., Carucci, N.M., Meli, G., Arisi, I., D'Onofrio, M., Marinelli, S., et al. (2018). NGF steers microglia toward a neuroprotective phenotype. *Glia* 66, 1395-1416.
- Li, X., Li, F., Ling, L., Li, C., and Zhong, Y. (2018). Intranasal administration of nerve growth factor promotes angiogenesis via activation of PI3K/Akt signaling following cerebral infarction in rats. *Am. J. Transl. Res.* 10, 3481-3492.
- Zhu, W., Cheng, S., Xu, G., Ma, M., Zhou, Z., Liu, D., and Liu, X. (2011). Intranasal nerve growth factor enhances striatal neurogenesis in adult rats with focal cerebral ischemia. *Drug Deliv.* 18, 338-343.
- Lee, T.H., Kato, H., Chen, S.T., Kogure, K., and Itoyama, Y. (1998). Expression of nerve growth factor and trkA after transient focal cerebral ischemia in rats. *Stroke* 29, 1687-1696, discussion 1697.
- Chiaretti, A., Antonelli, A., Genovese, O., Fernandez, E., Giuda, D., Mariotti, P., and Riccardi, R. (2008). Intraventricular nerve growth factor infusion improves cerebral blood flow and stimulates doublecortin expression in two infants with hypoxic-ischemic brain injury. *Neurol. Res.* 30, 223-228.
- Fantacci, C., Capozzi, D., Ferrara, P., and Chiaretti, A. (2013). Neuroprotective role of nerve growth factor in hypoxic-ischemic brain injury. *Brain Sci.* 3, 1013-1022.
- Aloe, L., Rocco, M.L., Bianchi, P., and Manni, L. (2012). Nerve growth factor: from the early discoveries to the potential clinical use. *J. Transl. Med.* 10, 239.
- Tria, M.A., Fusco, M., Vantini, G., and Mariot, R. (1994). Pharmacokinetics of nerve growth factor (NGF) following different routes of administration to adult rats. *Exp. Neurol.* 127, 178-183.
- Pan, W., Banks, W.A., and Kastin, A.J. (1998). Permeability of the blood-brain barrier to neurotrophins. *Brain Res.* 788, 87-94.
- EL Andaloussi, S., Mäger, I., Breakefield, X.O., and Wood, M.J. (2013). Extracellular vesicles: biology and emerging therapeutic opportunities. *Nat. Rev. Drug Discov.* 12, 347-357.

20. Yang, J., Zhang, X., Chen, X., Wang, L., and Yang, G. (2017). Exosome Mediated Delivery of miR-124 Promotes Neurogenesis after Ischemia. *Mol. Ther. Nucleic Acids* 7, 278–287.
21. Théry, C., Witwer, K.W., Aikawa, E., Alcaraz, M.J., Anderson, J.D., Andriantsitohaina, R., Antoniou, A., Arab, T., Archer, F., Atkin-Smith, G.K., et al. (2018). Minimal information for studies of extracellular vesicles 2018 (MISEV2018): a position statement of the International Society for Extracellular Vesicles and update of the MISEV2014 guidelines. *J. Extracell. Vesicles* 7, 1535750.
22. Valadi, H., Ekström, K., Bossios, A., Sjöstrand, M., Lee, J.J., and Lötvall, J.O. (2007). Exosome-mediated transfer of mRNAs and microRNAs is a novel mechanism of genetic exchange between cells. *Nat. Cell Biol.* 9, 654–659.
23. Skog, J., Würdinger, T., van Rijn, S., Meijer, D.H., Gainche, L., Sena-Esteves, M., Curry, W.T., Jr., Carter, B.S., Krichevsky, A.M., and Breakefield, X.O. (2008). Glioblastoma microvesicles transport RNA and proteins that promote tumour growth and provide diagnostic biomarkers. *Nat. Cell Biol.* 10, 1470–1476.
24. Li, Z., Zhou, X., Wei, M., Gao, X., Zhao, L., Shi, R., Sun, W., Duan, Y., Yang, G., and Yuan, L. (2019). In Vitro and in Vivo RNA Inhibition by CD9-HuR Functionalized Exosomes Encapsulated with miRNA or CRISPR/dCas9. *Nano Lett.* 19, 19–28.
25. Lai, C.P., Kim, E.Y., Badr, C.E., Weissleder, R., Mempel, T.R., Tannous, B.A., and Breakefield, X.O. (2015). Visualization and tracking of tumour extracellular vesicle delivery and RNA translation using multiplexed reporters. *Nat. Commun.* 6, 7029.
26. Lai, C.P., Mardini, O., Ericsson, M., Prabhakar, S., Maguire, C., Chen, J.W., Tannous, B.A., and Breakefield, X.O. (2014). Dynamic biodistribution of extracellular vesicles in vivo using a multimodal imaging reporter. *ACS Nano* 8, 483–494.
27. Yuan, D., Zhao, Y., Banks, W.A., Bullock, K.M., Haney, M., Batrakova, E., and Kabanov, A.V. (2017). Macrophage exosomes as natural nanocarriers for protein delivery to inflamed brain. *Biomaterials* 142, 1–12.
28. Hu, X., Leak, R.K., Shi, Y., Suenaga, J., Gao, Y., Zheng, P., and Chen, J. (2015). Microglial and macrophage polarization—new prospects for brain repair. *Nat. Rev. Neurol.* 11, 56–64.
29. Tuszyński, M.H., Yang, J.H., Barba, D., U, H.S., Bakay, R.A., Pay, M.M., Masliah, E., Conner, J.M., Kobalka, P., Roy, S., and Nagahara, A.H. (2015). Nerve Growth Factor Gene Therapy: Activation of Neuronal Responses in Alzheimer Disease. *JAMA Neurol.* 72, 1139–1147.
30. Lin, Y., Wan, J.Q., Gao, G.Y., Pan, Y.H., Ding, S.H., Fan, Y.L., Wang, Y., and Jiang, J.Y. (2015). Direct hippocampal injection of pseudo lentivirus-delivered nerve growth factor gene rescues the damaged cognitive function after traumatic brain injury in the rat. *Biomaterials* 69, 148–157.
31. Xu, D., Wu, D., Qin, M., Nih, L.R., Liu, C., Cao, Z., Ren, J., Chen, X., He, Z., Yu, W., et al. (2019). Efficient Delivery of Nerve Growth Factors to the Central Nervous System for Neural Regeneration. *Adv. Mater.* 31, e1900727.
32. Houlton, J., Abumaria, N., Hinkley, S.F.R., and Clarkson, A.N. (2019). Therapeutic Potential of Neurotrophins for Repair After Brain Injury: A Helping Hand From Biomaterials. *Front. Neurosci.* 13, 790.
33. Lapchak, P.A., Araujo, D.M., Carswell, S., and Hefti, F. (1993). Distribution of [125I] nerve growth factor in the rat brain following a single intraventricular injection: correlation with the topographical distribution of trkA messenger RNA-expressing cells. *Neuroscience* 54, 445–460.
34. Thorne, R.G., and Frey, W.H., 2nd (2001). Delivery of neurotrophic factors to the central nervous system: pharmacokinetic considerations. *Clin. Pharmacokinet.* 40, 907–946.
35. Petty, B.G., Cornblath, D.R., Adornato, B.T., Chaudhry, V., Flexner, C., Wachsman, M., Sinicropi, D., Burton, L.E., and Peroutka, S.J. (1994). The effect of systemically administered recombinant human nerve growth factor in healthy human subjects. *Ann. Neurol.* 36, 244–246.
36. Farooqi, A.A., Desai, N.N., Qureshi, M.Z., Librelotto, D.R.N., Gasparri, M.L., Bishayee, A., Nabavi, S.M., Curti, V., and Daglia, M. (2018). Exosome biogenesis, bioactivities and functions as new delivery systems of natural compounds. *Biotechnol. Adv.* 36, 328–334.
37. Armstrong, J.P., Holme, M.N., and Stevens, M.M. (2017). Re-Engineering Extracellular Vesicles as Smart Nanoscale Therapeutics. *ACS Nano* 11, 69–83.
38. Sahin, U., Karikó, K., and Türeci, Ö. (2014). mRNA-based therapeutics—developing a new class of drugs. *Nat. Rev. Drug Discov.* 13, 759–780.
39. Kauffman, K.J., Webber, M.J., and Anderson, D.G. (2016). Materials for non-viral intracellular delivery of messenger RNA therapeutics. *J. Control. Release* 240, 227–234.
40. Alvarez-Erviti, L., Seow, Y., Yin, H., Betts, C., Lakhali, S., and Wood, M.J. (2011). Delivery of siRNA to the mouse brain by systemic injection of targeted exosomes. *Nat. Biotechnol.* 29, 341–345.
41. Elsharkasy, O.M., Nordin, J.Z., Hagey, D.W., de Jong, O.G., Schiffelers, R.M., Andaloussi, S.E., and Vader, P. (2020). Extracellular vesicles as drug delivery systems: Why and how? *Adv. Drug Deliv. Rev.*, S0169-409X(20)30024-7.
42. Haney, M.J., Klyachko, N.L., Zhao, Y., Gupta, R., Plotnikova, E.G., He, Z., Patel, T., Piroyan, A., Sokolsky, M., Kabanov, A.V., and Batrakova, E.V. (2015). Exosomes as drug delivery vehicles for Parkinson's disease therapy. *J. Control. Release* 207, 18–30.